

Received 25 September 2023, accepted 24 October 2023, date of publication 30 October 2023, date of current version 7 November 2023.

Digital Object Identifier 10.1109/ACCESS.2023.3328778

RESEARCH ARTICLE

Application of Improved KAZE Algorithm in Image Feature Extraction and Matching

PEIPEI ZHANG¹ AND XIN'E YAN²

¹School of Zhong Xing Communication, Xi'an Traffic Engineering Institute, Xi'an 710300, China

²School of Civil Engineering, Xi'an Traffic Engineering Institute, Xi'an 710300, China

Corresponding author: Peipei Zhang (zhangpeipei928@163.com)

ABSTRACT Intelligent navigation and recognition technology have continuously improved the field of image matching, so how to achieve more efficient and accurate feature matching is the key to image processing. This study provides a detailed introduction to the calculation methods, advantages and disadvantages of various algorithms such as SIFT, ORB and KAZE. Finally, the KAZE algorithm was selected because it can better handle edge information. However, this algorithm still has drawbacks such as high computational cost. Therefore, starting from the feature description and similarity calculation, the study introduced the concepts of second-order degree values, circular rotation characteristics, and expected distance and intercept distance to improve it, which is called the algorithm. Theoretically, this algorithm can greatly reduce the computational burden of the algorithm. To further validate the effectiveness of the improved algorithm, the study selected five types of image groups from the Mikolajczyk standard image database, including changes in image scale, brightness, and perspective. Simulation experiments were conducted on the improved algorithm and the remaining five algorithms. The experimental results show that compared to the original algorithm, Li-KAZE reduces the overall running time by 27.9% and improves the average matching rate by 0.12%. Compared to other SIFT and other algorithms, Li-KAZE also has the best performance among all algorithms. When faced with changes in compression values and extensive changes in graph groups, its highest repeatability reaches 99%. In summary, the comprehensive performance of the Li-KAZE algorithm has achieved the goal of improvement.


INDEX TERMS Feature extraction, image matching, KAZE algorithm, scale space, nonlinear filtering.

I. INTRODUCTION

Images, as the most common carrier of information transmission, are accompanied by a huge data system. According to statistics, visual images account for about 75% of the information received by each person [1]. Therefore, intelligent recognition of images is the current research hotspot. Computer images can be divided into analog images and digital images, the difference between the two lies in the form of data recording. The former is based on changes in specific physical quantities, while the latter is stored in computerized form. In image processing, digital image formats are usually used and various algorithms are selected as needed to achieve the desired results. In the past, image processing was mainly

concerned with improving the visual appearance of an image by altering its sharpness and other factors. Nowadays, image processing techniques have been developed on more levels, including image segmentation, feature matching, geometric processing, etc., which can be applied in many fields such as military, agriculture, and medicine.

Image matching is an important part of the whole image processing field, aiming to utilize some kind of technology to achieve feature matching between multiple images. Nowadays, the common virtual simulation, face recognition and three-dimensional reconstruction, etc., all belong to the image matching technology, so it can be seen that the importance of image matching for human daily life work. The traditional pixel-based matching method is often easily affected by factors such as brightness and image ratio, and cannot complete the matching successfully. Therefore, local feature

The associate editor coordinating the review of this manuscript and approving it for publication was Jon Atli Benediktsson .

point-based matching techniques are often used nowadays to better cope with the interference of the external environment [2]. The basis of feature matching is feature extraction, and the basic framework of these two processes is roughly the same, both of which require the establishment of a scale space. The purpose of establishing a scale space before feature extraction is to preserve the scale information of the original image and avoid the problem of oversimplification. Proportion spaces can be categorized as linear or nonlinear. Linear structures are usually accomplished by using Gaussian filters. Although most of the scale can be preserved, the data information of certain details is still not accurate enough, and the final image matching effect is poor. Nonlinear scale space effectively solves this problem and can make the image matching results more accurate [3].

Scholars in this field have been committed to improving the robustness of image feature extraction and matching, and have also achieved certain results. However, there is almost no method, which can simultaneously cope with multiple composite interference situations such as light intensity, scale transformation, noise and distortion, and at the same time have real-time characteristics. To solve this phenomenon, this study proposes an image matching technique based on the improved Li-KAZE algorithm. The full text is mainly divided into four parts. The first part introduces the application of image matching algorithm at home and abroad. The second part introduces the basic principles of image feature extraction and matching, analyzes and compares several commonly used algorithms, and finally selects the most suitable KAZE algorithm. Meanwhile, the concepts of second-order degree value (2ndODV), circular rotation characteristic (CRC), expected distance and intercept (BD-CD) are introduced to improve the computational complexity of the original algorithm. The third part compares the improved Li-KAZE algorithm with other algorithms to verify its effectiveness. Finally, the experimental results are summarized in Part IV. The nonlinear scale space adopted in the study solves the problem that a large number of image matching algorithms are unable to cope with changes in the scale of images, while further improving the retention of detailed image features. All abbreviations are shown in Table 1.

II. RELATED WORKS

Research is constantly deepening, and image matching technology is also constantly improving. Liu et al. applied the AKAZE algorithm to glass encapsulated electrical connectors, but its image matching effect was poor. Therefore, scholars have introduced the concepts of Lucas-Kanade (LK) optical flow and grid motion to improve it by restricting feature points and selecting appropriate matching points from them. By combining the Fast Library for Approximate Nearest Neighbors (FLANN) algorithm, the problem of excessive computational burden in the original algorithm was improved. The improved algorithm achieved a matching accuracy of over 93% and consumed only 0.4s [4]. Al Shurbaji et al. used scale invariant features to achieve

TABLE 1. Abbreviations for each name.

Content	Parameter
Lucas – Kanade	LK
Fast Library for Approximate Nearest Neighbors	FLANN
Principal Component Analysis	PCA
Random Sample Consensus	RANSAC
Graphical Modeling System	GMS
Second-order gradient information	2NDODV
Circular rotation characteristics	CRC
Block distance-Checkerboard distance	BD-CD
Scale-invariant Feature Transform	SIFT
Speed Up Robust Features	SURF

feature matching, but their embedded computing format significantly increased the computational burden. Therefore, scholars have proposed the chamfer distance algorithm to improve it. Compared with the traditional Euclidean distance measurement method, this algorithm can directly select the shortest distance between any two points, thus achieving shorter computation time. Finally, simulation experiments have verified that the algorithm reduces the computation time by 41% compared with the original algorithm [5]. Yan et al. proposed a capacitance tomography imaging technique to improve image quality to achieve better image matching results, which is achieved by orthogonal matching tracking. This involved selecting multiple columns during iteration to improve the construction time. Meanwhile, the least squares solution was replaced with the regularization solution, which greatly improves the adaptability of the system, and the effectiveness of this method is verified [6]. Yue et al. introduced a fast image matching algorithm to construct affine invariant, which can obtain the diversity of multiple image features. And it also solved the algorithm failure defects commonly found in affine geometric features, improved matching accuracy, and overcame shortcomings such as contour problems and overlap failure. The speed-up ratio of this algorithm has reached about 1.75 times that of the original algorithm [7].

Liang et al. applied the local feature point extraction algorithm to the matching of deep color images, achieved the matching by local feature point extraction of two types of images and optimized the affine transform matrix on this basis, and the experimental results show that the accuracy of their algorithm is 15 times higher than that of the rest of the three algorithms on average, and it has a high degree of accuracy and effectiveness [8]. Ji et al. conducted a comparative analysis of traditional image matching methods and deep learning based image matching methods by following three steps of feature extraction, feature description, and similarity computation, and the experimental results show that the effect of dataset on the model is significant, while the efficiency of the deep learning method is to be improved [9]. Ding et al. proposed a new image matching algorithm by combining the concepts of vector coefficient similarity, graph cut random sample consistency, and grid motion statistics. In the initial stage, the ORB algorithm was used to extract and match the feature points, and then the Graphical Modeling

System (GMS) algorithm was used to further fine match the features. The similarity of vector coefficients does not exceed the set threshold rule, which can speed up the convergence speed in the later stage of calculation; The graph-cut random sample consistency algorithm is used to fit the local best model, making the feature set more accurate. Experiments have shown that, compared with other algorithms mentioned in this theory, the new algorithm has an average increase in matching accuracy of 30.34% and a reduction in computation time of about half a second [10]. Qian et al. believed that the key to binocular stereo matching methods lies in the detection of occluded regions. However, traditional methods require high accuracy in left and right disparity maps and cannot detect edge information of images. The new detection method proposed in this study can detect the occluded part of a single image, thus greatly reducing the computational burden. It can also better identify the occluded parts of the whole image set, and the filter has also been improved to further enhance the performance of the algorithm [11].

A large number of studies have shown that the computational amount is too large, as well as the extraction and matching process is susceptible to the interference of external conditions, which is a common defect of the current feature matching algorithm, and for the solution of this defect, the feature extraction technology and the innovation of the matching method are more critical. Based on this, the study proposes a matching technique based on the optimized KAZE algorithm, which makes use of its constructed nonlinear scale space and Second-order gradient information (2ndODV) to achieve higher noise immunity and non-deformation to improve the accuracy of feature extraction; and chooses the Block Distance-Checkerboard Distance (BD-CD) instead of the traditional Euclidean Distance for similarity measurement, which greatly reduces the computational burden of the model.

III. APPLICATION OF IMPROVED KAZE ALGORITHM IN IMAGE FEATURE EXTRACTION AND MATCHING

A. THE PROCESS DESIGN OF IMAGE FEATURE EXTRACTION AND MATCHING AND THE OPERATION MECHANISM ANALYSIS OF EACH ALGORITHM

Image matching technology based on feature extraction is currently one of the most powerful methods in the field of image recognition. The commonly used feature extraction algorithms include Scale-invariant Feature Transform (SIFT), Speed Up Robust Features (SURF), Oriented FAST and Rotated BRIEF (ORB), and KAZE algorithm. The SIFT feature is an algorithm that solves the problem of accuracy degradation caused by size changes. This algorithm adopts the method of constructing a scale space to visualize the scale features of the image, which avoids the problem of unstable retrieval values when the size angle of the image changes [12]. In accordance with previous research experience, the scale space can be regarded as the convolution of the original image and the Gaussian function, and its expression is

formula (1):

$$L(x, y, \sigma) = G(x, y, \sigma) * I(x, y) \tag{1}$$

In equation (1) above, $L(x, y, \sigma)$ represents the constructed scale space; $G(x, y, \sigma)$ is a function of Gaussian kernel σ ; $I(x, y)$ is the input image; $*$ represents the convolution operator. Scholars use DoG operators similar to LoG operators for feature extraction, which can achieve higher feature invariance. Finally, each neighboring layer is subtracted separately to obtain a Gaussian difference pyramid as Figure 1:

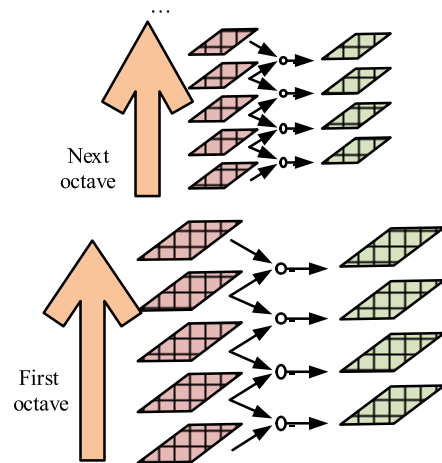


FIGURE 1. Gaussian pyramid.

Set the pyramid to contain a total of O sets of images, with each set containing S layers. In general, the value of S is a natural number between 3 and 5. The first images of each set are obtained by downsampling the original image in order. Although the simulation of image scale changes can be achieved, it also greatly increases the computational burden of the algorithm. And when selecting extreme points, it is necessary to satisfy the extreme requirements of both the current layer and the adjacent layers simultaneously. The above content is the preliminary detection and selection process of feature values, and the final feature points still need further screening and positioning. At the same time, to eliminate the matching error caused by image rotation, each feature value contains a corresponding main direction, which must be determined by the peak value of its neighboring gradient histogram [13]. The final generated feature vector is shown in Figure 2:

As Figure 2, the basic elements of key points include direction, position, and scale. Divide key points to obtain a total of $4 \times 4 = 16$ sub blocks, each containing 8 gradient values in different directions, ultimately resulting in $16 \times 8 = 128$ dimensions of data information. SURF algorithm uses the Hessian matrix value to detect feature points and further operate. The relationship expression of Hessian matrix in two-dimensional space is formula (2):

$$H(x, \sigma) = \begin{bmatrix} L_{xx}(x, \sigma) & L_{xy}(x, \sigma) \\ L_{xy}(x, \sigma) & L_{yy}(x, \sigma) \end{bmatrix} \tag{2}$$

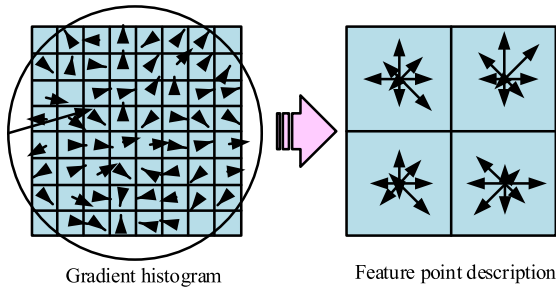


FIGURE 2. Feature vectors generated by gradient histogram.

In equation (2), L represents the second-order Gaussian convolution value with image $I(x, y)$ in a certain direction. The calculation process of this algorithm is relatively simple and does not require changing the scale of the original image, but rather changes with the size of the Gaussian template. The emergence of SIFT algorithm solves the problem of image scale change, and the introduction of its pyramid structure and main direction effectively solves the problem of image scale and angle transformation. However, due to the limitations of its feature extraction method, the algorithm has poor performance in timeliness. Thus, the SURF algorithm runs faster than the SIFT algorithm that requires downsampling. This algorithm uses wavelet transform to select the main direction of feature points, as shown in Figure 3:

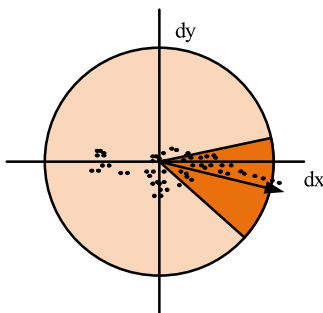


FIGURE 3. Main direction selection.

From Figure 3, the center of the circle is selected as the location of the key point, and the feature point scale is used as the radius, followed by equal segmentation according to a width of 60° . The Hale wavelet response values of each sector are counted, and the direction with the longest vector is selected as the main direction of the feature point, which is divided into 20 seconds around the main direction region of $20s \times 20s$, making a total of 16 sub regions. Finally, the weights of each direction in the sub-region are calculated by wavelet transform. The computational complexity of this algorithm is greatly reduced. Therefore, SURF algorithm is equivalent to SIFT algorithm optimized in timeliness. The ORB algorithm has a more significant improvement in computational speed compared to the above algorithms. This is because the ORB algorithm uses the principle of the FAST algorithm to achieve feature detection by adding the

corresponding main direction when describing the features, hence it is also called oFAST, and the feature vectors all use binary feature vectors of 0 or 1. Theoretically, the study selects pixels with a certain difference in gray values from their neighbors as corner points. The actual operation is shown in Figure 4:

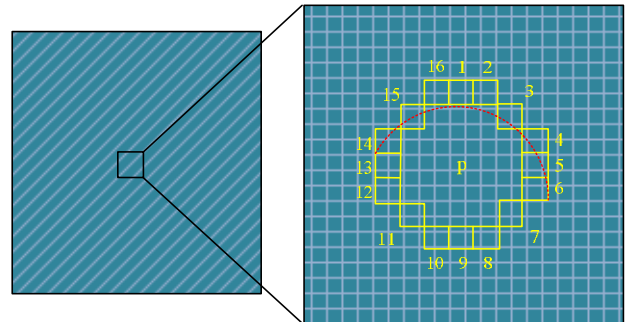


FIGURE 4. ORB algorithm.

From Figure 4, first, any pixel point P is used as a circle, and 3 is used as the radius value. Therefore, this point contains a total of 16 adjacent pixel points. When there are up to n points in the neighboring points that meet the gray level difference greater than t condition compared to point P , point P can be considered as a key point. To further enhance the algorithm's running speed, the algorithm adopts segmented judgment to reduce unnecessary computational waste, but there is still a problem of reduced eigenvalue independence in this algorithm. It can be seen that ORB algorithm introduces FAST algorithm to improve the operation efficiency. At the same time, it also uses the addition of Gaussian image pyramid and the main direction of the center of mass to solve the defects of FAST algorithm in the face of images with scale changes and rotation changes, but the distinguishable stars of descriptors in the algorithm are reduced. The final algorithm is the KAZE algorithm, which is based on a nonlinear scale space. Unlike the SIFT algorithm, which requires a stepwise downsampling of the linear scale space, this nonlinear scale space is easier to construct. The scale parameter calculation is given by formula (3):

$$\sigma_i(o, s) = \sigma_0 2^{o+s/S} \tag{3}$$

In equation (6) above, o represents the group number, with a range between $[0 \dots O - 1]$; s presentation layer number, ranging from $[0 \dots S - 1]$; Image i is between $[0 \dots N]$, and $N = O \times S$ represents the total number of images; σ_0 represents the benchmark value of the scale parameter. The conversion formula between the scale parameter σ_i of a certain pixel and the evolution time t_i is formula (4):

$$t_i = \frac{1}{2} \sigma_i^2, i \in \{0 \dots N\} \tag{4}$$

Feature extraction is a key step in image matching. Image features can be divided into global features and local features according to their properties. Global representation of the

overall description, commonly including color and texture information and other feature data, such features are mostly used for searching and tracking of a certain target, but in the processing of detail data and other refined areas, but poor performance, especially the shadow shading problem, will greatly reduce its performance. Local features, on the other hand, are more suitable for processing local details. Features contain information about themselves and neighboring feature points. Feature points typically appear at locations with large gray level changes and represent the intended points, crosspoints, or corner points of the image, ensuring that the probability of occurrence of these points remains high even as the scale or ambiguity of the image changes. This also lays the foundation for the application of local features to image matching. In this study, the local feature of the dot is selected as the object of investigation. For each algorithm, the basic feature extraction process is roughly the same. First, global detection of image feature points is required. The difference between algorithms lies in the description of the feature points, so the feature points detected by different algorithms will also be different. Then the description of the feature, the algorithm will process the image block near the feature point and describe it according to the information.

According to the previous experimental analysis, in terms of preserving the original image features, the nonlinear diffusion filter performance is better than the traditional Gaussian filter, which can preserve the edge and detail features of the original image to a greater extent. Usually, for different image features, it is necessary to choose different matching methods to achieve image correlation retrieval. However, camera performance, azimuth angle, and various environmental factors can affect the image, causing changes in its original features and ultimately leading to image matching failure. This is also one of the major reasons hindering the development of image matching technology. Therefore, eliminating irrelevant elements, extracting reliable contrastive features from images, and achieving more accurate matching effects are currently the key and difficult points to be overcome. The current image matching technology roughly includes two categories: feature based and grayscale based. The basic process of the algorithm based on feature matching is Figure 5:

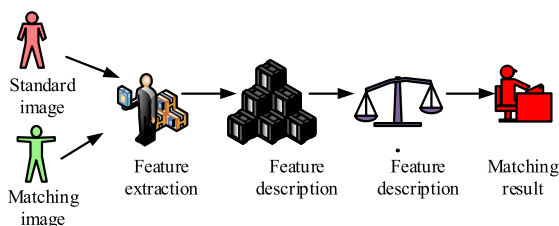


FIGURE 5. Feature matching process.

This method can effectively eliminate the influence of noise factors and maintain stable feature sizes. The grayscale information algorithm uses the comparison of image grayscale values on pixels to achieve matching, but this

type of algorithm is highly susceptible to noise and image scale interference in information detection [14]. Thus, the research ultimately selected the KAZE algorithm for feature extraction, and provided a detailed description of the algorithm and its improved algorithms.

B. OPTIMIZATION AND FEATURE MATCHING DESIGN OF KAZE ALGORITHM

The KAZE algorithm uses nonlinear diffusion filtering, which is a digital image processing technology that combines partial differential equations. Similar to the heat balance theory in physics, when the grayscale values in an image change, the original grayscale balance state is broken, causing the gray content to flow from the high grayscale range to the low grayscale range. This can greatly reduce the grayscale changes of the whole image, stabilize it, and finally achieve the noise reduction function, becoming a constant value image [15]. Other algorithms usually use a Gaussian filter with a fixed diffusion coefficient of 1, which makes it lose the original details while smoothing the image. The nonlinear diffusion filtering algorithm used in this study can preserve edge features through anisotropy because its diffusion coefficient can change with gradient. The commonly used PM diffusion equation is formula (5):

$$\begin{cases} \frac{\partial L}{\partial t} = \text{div}(c(x, y, t) \cdot \nabla L) \\ c(x, y, t) = g(|\nabla L_\sigma(x, y, t)|) \end{cases} \quad (5)$$

In equation (5), L represents the grayscale value; t represents the scale parameter, and the larger the value, the simpler the image; $c(x, y, t)$ represents the conduction function, which determines whether diffusion can achieve adaptive function, where the smoothing effect of the image is positively correlated with the t value; The expression of the function is expressed in formula (6):

$$g_1 = \exp\left(-\frac{|\nabla L_\sigma|^2}{k^2}\right)$$

$$g_2 = \frac{1}{1 + \frac{|\nabla L_\sigma|^2}{k^2}}$$

$$g_3 = \begin{cases} 1, & |\nabla L_\sigma|^2 = 0 \\ 1 - \exp\left(-\frac{3.315}{(|\nabla L_\sigma|/k)^8}\right), & |\nabla L_\sigma|^2 > 0 \end{cases} \quad (6)$$

In Eq.(6), ∇L_σ represents the gradient of the Gaussian smooth image; k represents the diffusion factor. The diffusion centers of the three g -functions are different. The g_1 -function determines whether the edges are retained based on contrast, the g_2 -function determines by width, and the g_3 -function determines whether the edges are prioritized by detecting whether the image is smooth. The KAZE algorithm selects a g_2 function based on width value diffusion. The larger the diffusion control factor k in the function, the less edge information is retained. Although the performance of nonlinear filtering is better than that of Gaussian filter, it has not

been dominant in the research. This is because the forward Euler method method is usually used for nonlinear filtering, which requires a large amount of computation, resulting in a great discount in the efficiency of the algorithm. Therefore, the KAZE algorithm adopts the Additive Operator Splitting (ASO) algorithm, the convergence step of which can be set arbitrarily, and ultimately obtains a more stable scale space [16]. Due to the lack of solutions for nonlinear partial differential equations, this study combined them with the Thomas algorithm to obtain an approximate difference equation as expressed in formula (7):

$$\frac{L^{i+1} - L^i}{\tau} = \sum_{l=1}^m A_l(L^i)L^{i+1}x \quad (7)$$

In Eq. (7), A_l represents the conductivity matrix of three diagonals. Scale space can eliminate the problem of inaccurate matching caused by changes in image scale. Unlike traditional scale space construction, the KAZE algorithm changes from linear to nonlinear. The basic steps of the two construction methods are similar, but the KAZE algorithm omits the downsampling link, and its image resolution remains unchanged. The scale parameter σ_i is expressed in Formula (8) [17]:

$$\sigma_i(o, s) = \sigma_0 2^{o+s/S}, o \in [0 \dots O - 1], s \in [0 \dots S - 1], i \in [0 \dots N] \quad (8)$$

In equation (8), o represents the group number; s presentation layer number; σ_0 represents the benchmark scale parameter; Number of images $N = O \times S$. σ_i is different from the dimension of evolution time t_i , so the conversion process shown in formula (9) is required:

$$t_i = \frac{1}{2} \sigma_i^2, i \in \{0 \dots N\} \quad (9)$$

The image information obtained using AOS algorithm preserves the original edge and detail features more completely. The KAZE algorithm uses the Hessian matrix to detect the feature points, as displayed in formula (10):

$$L_{Hessian} = \sigma^2(L_{xx}L_{yy} - L_{xy}^2) \quad (10)$$

Its retrieval strategy is similar to the SIFT algorithm, following the order of 3×3 neighborhood comparison method to find extreme values. Then, according to the Taylor expansion, sub pixel locking is achieved, as listed in formula (11):

$$\begin{cases} L(x) = L + \left(\frac{\partial L}{\partial x}\right) + \frac{1}{2}x^T \frac{\partial^2 L}{\partial x^2}x \\ \hat{x} = -\left(\frac{\partial^2 L}{\partial x^2}\right)^{-1} \frac{\partial L}{\partial x} \end{cases} \quad (11)$$

The descriptor subconstruction of the KAZE algorithm is based on the construction concept of the SURF algorithm. Firstly, wavelet changes are used to partition each sector, and the longest vector is selected as the main direction. Then, Gaussian weighting is used to achieve the vector description of the sub regions, as listed in formula (12):

$$d_v = \left(\sum L_x, \sum L_y, \sum |L_x|, \sum |L_y|\right) \quad (12)$$

After selecting the key points of each image, correlation matching can be performed. The algorithm combines Euclidean distance and Ratio ratio to compare each feature value, and the specific process is Figure 6:

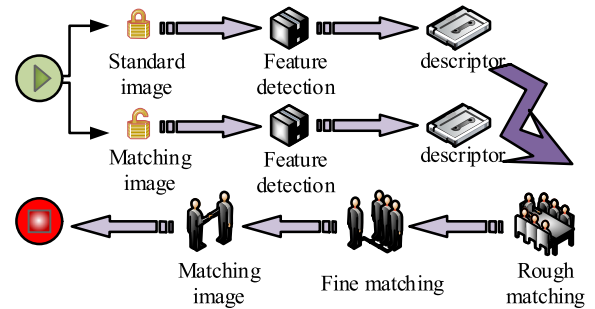


FIGURE 6. Process of image feature matching.

In Figure 6, the key to the matching process lies in detecting key points that match any feature-point-P in the standard image N in the image M to be matched. The Euclidean distances from all points in Figure 6 to feature-point-P are calculated by dividing the closest value by the value of the next closest distance: if the value is less than a fixed value, it indicates that the point is the correct matching point. By repeatedly performing the above calculations, a coarse match between two images can be obtained, and finally, accurate image matching can be further achieved using the RANSAC algorithm [18]. Although the KAZE algorithm can more accurately implement the image matching process, its computational burden is too high and its efficiency is not high enough. Therefore, a new Li-KAZE algorithm is proposed, which focuses on feature description and similarity calculation to reduce the computational burden of the algorithm. The calculation process is shown in Figure 7.

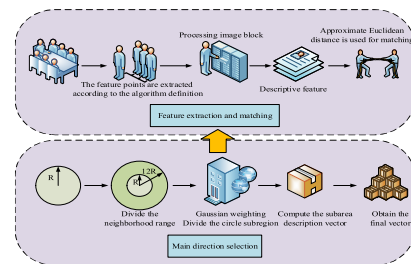


FIGURE 7. Overall operation flow of Li-KAZE optimization algorithm.

In the original KAZE algorithm, the rotation invariant M-SURF method is usually used to describe features. This method requires multiple iterations of the entire neighborhood data to select the principal direction and eigenvectors. This is usually done in the form of a sector window, and it is also necessary to count the feature vectors generated from the one-dimensional data in the neighboring regions. It can be seen that the traversal of the M-SURF method involves extracting the main direction and generating feature vectors. Its inherent high dimension further increases the calculation

load of the whole model, and only using Euclidean distance for feature matching will greatly reduce the timeliness of the model. Thus, the study used 2ndODV and Circular rotation characteristics (CRC) to improve it, and proposed a similarity analysis method combining BD-CD [19]. Among them, the main direction in the extraction step corresponding to the circular rotation feature is the M-SURF method. Unlike the original algorithm, it is lengthy and directly traverses all data. The improved algorithm first selects points that can be used as feature points as the center of the circle, sets the neighborhood range to a circle with a radius of 12 scale parameters, and sets the Gaussian weighting to 2.5. It is then partitioned into 5 circular subregions by a Gaussian weighting value of 2.5, and the calculation formula for the description vector of each sub region is formula (13):

$$d = \left(\sum L_x, \sum L_y, \sum |L_x|, \sum |L_y|, \sum L_{xx}, \sum L_{yy}, \sum |L_{xx}|, \sum |L_{yy}| \right) \quad (13)$$

In Eq. (13), L_x and L_y represent the first-order differentiation of the filtered image; L_{xx} and L_{yy} represent the second-order derivative of the filtered image; The rest represent the absolute values of their corresponding values. It is known that each vector is 8-dimensional, and after normalization, the $5 \times 8=40$ dimensional feature vectors can be obtained. The rotation invariance of a circle has the same function as the main direction, both in order to preserve the original data information when the image is flipped. The second-order gradient, on the other hand, is designed to more accurately describe the detailed features of an image, such as texture, including features at its edges. The nonlinear scale itself is good at dealing with noisy data, and the introduction of the second-order gradient concept can further assist in preserving the detailed features of the nonlinear scale space and enhance the attributes of the new features. Street distances are calculated in a way that approximates the length of streets with only 90 degree corners, so higher dimensional Spaces can sometimes achieve better results than Euclidean distances. The chessboard distance is the value of the largest absolute difference between two numerical vectors in a single dimension, so it is of great physical significance in some special scenes, such as in the process of assembling an item, many parts are needed, and each part needs to be mailed from different places, and the chessboard distance is the shortest time needed. The calculation of street distance L_1 , Euclidean distance L_2 , and chessboard distance L_∞ mentioned above is formula (14) [20]:

$$\begin{cases} L_1(x, y) = \sum_{i=1}^n |x_i - y_i| \\ L_2(x, y) = \left[\sum_{i=1}^n (x_i - y_i)^2 \right]^{\frac{1}{2}} \\ L_\infty(x, y) = \max_{1 \leq i \leq n} \{|x_i - y_i|\} \end{cases} \quad (14)$$

In equation (14) above, n represents the dimension of space; (x, y) represents two different points in the space. Based on the above formulas, it can be seen that the computational burden of the Euclidean distance is relatively greater. As for $L_\infty < L_2 < L_1$, the study utilizes the linear sum of the neighborhood distance and the checkerboard distance $\alpha(L_\infty + L_1)$ to indirectly obtain an approximation of the Euclidean distance. It is essentially the analogous relationship between the high-dimensional hyperpolyhedron and the hypersphere in geometry. The specific calculation is formula (15):

$$\begin{cases} L_2 = \alpha(L_\infty + L_1) \\ \alpha = \begin{cases} \left| \frac{2^n(n)!!}{2^{\frac{n+1}{2}} \pi^{\frac{n-1}{2}} (n+1)!} \right|^{\frac{1}{n}}, n \in (1, 3, 5, 7 \dots) \\ \left| \frac{2^n(\frac{n}{2})!!}{\pi^{\frac{n}{2}} (n+1)!} \right|^{\frac{1}{n}}, n \in (2, 4, 6, 8 \dots) \end{cases} \end{cases} \quad (15)$$

In equation (15) above, n represents the vector dimension, and the new feature dimension is known to be 40, therefore $n = 0.035$. The optimal solution of the coefficients α is a guarantee for improving the correctness of feature matching in the algorithm. The overall operation flow of Li-KAZE algorithm is shown in Figure 7.

IV. SIMULATION

A. BASIC PERFORMANCE ANALYSIS OF IMPROVED ALGORITHMS IN DIFFERENT DATA SETS

To further understand whether the performance of the improved KAZE algorithm can achieve the expected results in practical applications, performance simulation were conducted on it. The experimental environment is listed in table 2:

TABLE 2. Experimental environment.

Content	Parameter
Operating system	Windows 10
CPU	2.4GHz
GPU	NVIDIA Jetson TX2
Memory	8G
Programming environment	VS2015+Opencv3.1.0
Data set	Mikolajczyk

In this paper, a Graphic Processing Unit (GPU) is embedded in the computer to carry out constraints, which replaces the calculation of pixels, shadows and vertices in the original graphics. GPU is essentially a collection of graphics functions implemented by computer hardware, and this embedded device improves the time constraint of the computer to some extent. The experimental dataset was obtained from the Mikolajczyk standard image database. The gallery contains eight different sets of images, each of which contains an initial image, and five images subjected to artificial affine transformations. Therefore, the Affine transformation matrix can be used to obtain the matching position points, and the Euclidean distance between the correct matching point obtained through calculation and the matching point actually calculated by the

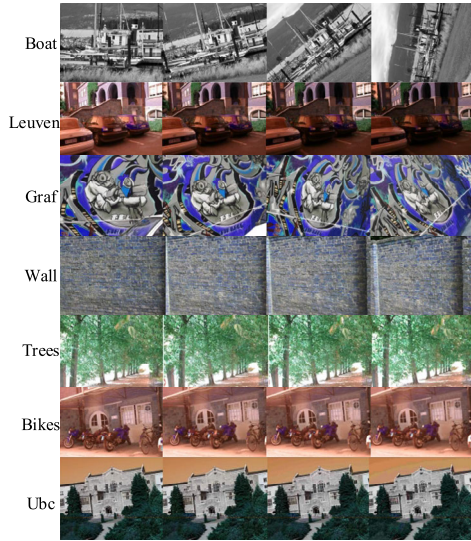


FIGURE 8. Total number of eigenvalues detected by the original algorithm and the improved algorithm.

algorithm is less than the threshold value. This means that the points matched by the algorithm are correct, and each set of data is tested using the first four images. The whole image library contains a variety of common forms of image transformations such as scale, view angle, illumination, etc., which is very suitable for performance testing of image matching algorithms. Among them, the Ubc set in the image library with changed image compression values can be used for the comparison of matching speeds of algorithms, but it is necessary to maintain the same hardware environment; The Bark dataset that changes the rotation angle can be used to compare the robustness of matching algorithms to rotated images. Because angle changes can also cause changes in pixel gradients and the main direction of feature points. At the same time, the dataset has undergone scale transformations, often resulting in new feature points. This is because angle transformation can also cause changes in pixel gradients and the main direction of feature points, and in this set of transformations, the scale size is also changed, often resulting in new feature points. This puts forward higher requirements for the matching performance of the algorithm. The Bikes group that changes the image resolution can be used to compare the robustness of matching algorithms in the face of fuzzy transformation images, and the resolution is inversely proportional to the algorithm performance. The Leuven group that changes the light intensity can be used to compare the robustness of the algorithm in different Grayscale. This is because the intensity of light can change the intra class scattering of the image, and the shaded parts may also cause key point occlusion, leading to a decrease in its matching performance; The Graf atlas with changing viewpoint information often leads to the loss of original image feature points. The Mikolajczyk image library selected in this study contains various common image feature transformation modes, which is very suitable for the study of

model recognition performance in the face of image changes, and can study the matching performance of the model in various aspects of feature changes. The seven selected image groups for the experiment were: Bikes; Wall; Graf changing perspective; Leuven changing the intensity of light; Trees that change clarity; Ubc changing the compression value and the Boat changing the scale. The above diagram group is shown in Figure 8.

The experiment first compared the performance of the initial KAZE with the improved Li KAZE, and the results of the feature points detected by the two algorithms are displayed in Figure 9:

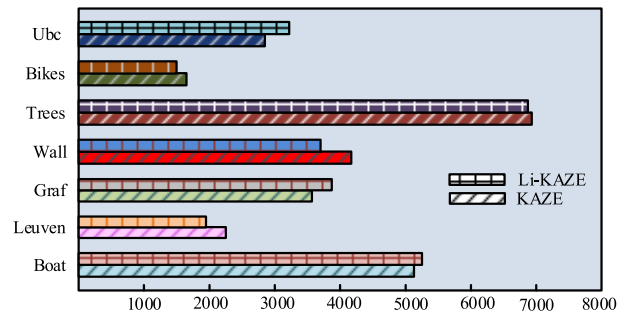


FIGURE 9. Total number of eigenvalues detected by the original algorithm and the improved algorithm.

In Figure 9, Li KAZE detected more feature points in Boat, Graf, and Ubc. That is, the improved algorithm can more accurately and as many matching feature points as possible when faced with changes in perspective, compression value, and scale. Although the number of feature points found in other graph groups is slightly insufficient, the performance research of the algorithm must not only compare the feature points, but also further analyze the efficiency of the algorithm based on accuracy. The comparison results of the detection time between the two algorithms are shown in Figure 10:

From Figure 10, both algorithms have insufficient detection efficiency for trees with altered clarity. However, overall, the feature detection time of Li-KAZE is lower than that of the original algorithm in almost all graph groups. Among them, Li-KAZE achieved the minimum feature detection time of only 2 seconds in Ubc. And in Boat, Trees, and Ubc, Li-KAZE increased by 0.13 seconds, 0.2 seconds, and 0.12 seconds compared to KAZE, respectively. Even when facing trees with unsatisfactory results, improved algorithms can significantly improve detection efficiency. The average feature detection time of the initial algorithm in all graph groups is 2.43 seconds, while that time of Li-KAZE is 2.33 seconds. Therefore, its ability to achieve a reduction in feature-detection time is due to the structure of Li-KAZE, which can greatly reduce the computational burden of the algorithm and has higher stability. The key steps to achieve image retrieval also include feature matching, and the feature matching time results of the two algorithms are in Figure 11:

From Figure 11, compared to the performance of feature detection, the improved algorithm has a more significant

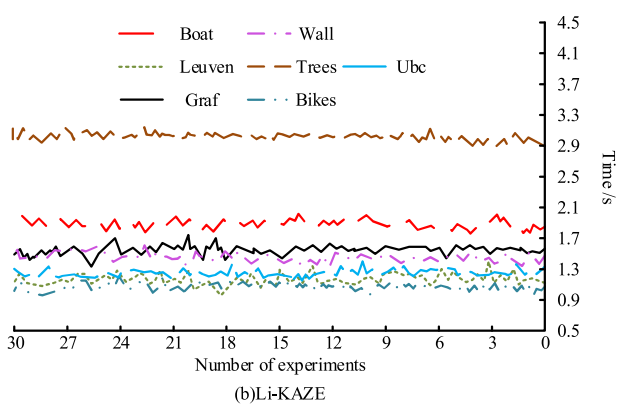
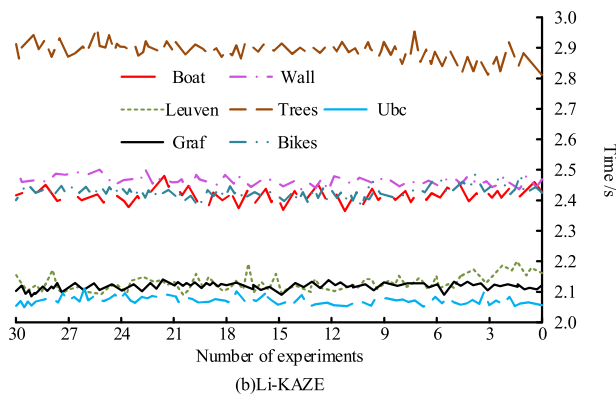
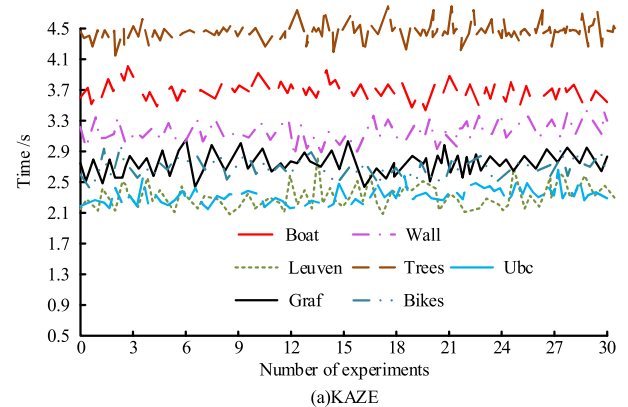
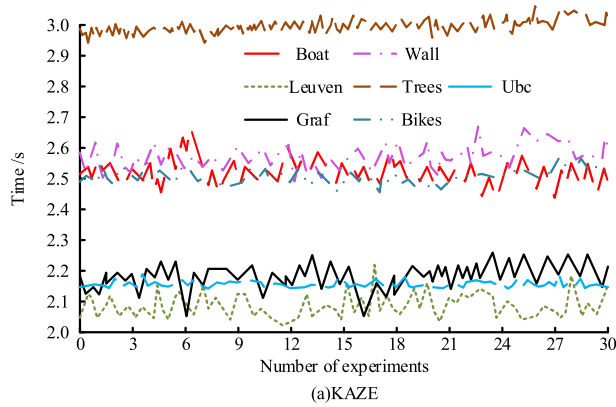


FIGURE 10. Comparison of feature detection time.

FIGURE 11. Feature matching time comparison.

performance improvement in the feature matching speed, with a matching time of only 1.0s in Bikes. The average matching time of all graph groups is 1.57s, and only in trees does the matching time exceed two seconds, reaching 2.98s, which is a decrease of 1.42s compared to the original graph group’s 4.4 seconds. The average matching time of the initial algorithm is 3.01s, which is 1.44s longer than the improved algorithm. In addition, the matching time of LI-KAZE has been reduced by more than 1 second in each graph group, and by as much as 1.9 seconds in Boat. Therefore, compared with the original KAZE, the improved Li-KAZE has a faster feature matching speed, which achieves the goal of improving the original algorithm. In addition, the image matching accuracy is also an important indicator to evaluate the algorithm performance, as shown in Figure 12:

From Figure 12, the final matching accuracy of the two algorithms is not significantly different, but the improved algorithm can learn faster, reduce the training time of the algorithm, and accelerate the speed of accuracy improvement. And by combining the number of feature-points and feature-detection matching time indicators in the above figure, it can be concluded that the comprehensive performance of Li-KAZE has been significantly improved, reducing computational burden, and having advantages in more datasets. The matching accuracy of Li-KAZE in bicycles reached 98.2%, with an average matching accuracy of 0.94, an improvement of 0.12% compared to the original algorithm, and it reduced

the total computation time of the original algorithm by 27.9%. In summary, Li-KAZE has better performance and faster computation speed than the original KAZE.

B. COMPARATIVE ANALYSIS OF THE PERFORMANCE OF THE IMPROVED ALGORITHM UNDER DIFFERENT IMAGE TRANSFORMATION FORMS

To further verify the excellent performance of the algorithm in other algorithm types, the study conducted several comparative analyses between the above two algorithms and four algorithms, including SIFT, ORB, and SURF. Due to the excessive number of algorithm types and graph groups, this study appropriately reduced the number of experiments per graph group. The experimental results of changing the clarity and scale of image groups are in Figure 13:

Figure 13(a) shows that the BRIEF algorithm has the worst performance, with the highest repeatability of only 19% in bicycles; The highest repeatability of Li-KAZE reached 91%, an increase of 72%. And the descent speed of Li-KAZE is also relatively slow and overall relatively smooth. For algorithms such as ORB, although the initial repeatability rate is 61%, the overall trend of change is relatively steep, with fast and rapid changes, and the final repeatability rate is only 27%. Therefore, among the wheels with changing ambiguity, Li-KAZE has the best repeatability performance. In fig. 13(b), in Boat with changed image scale, BRIEF is still in the worst position, with a steeper overall change and lower

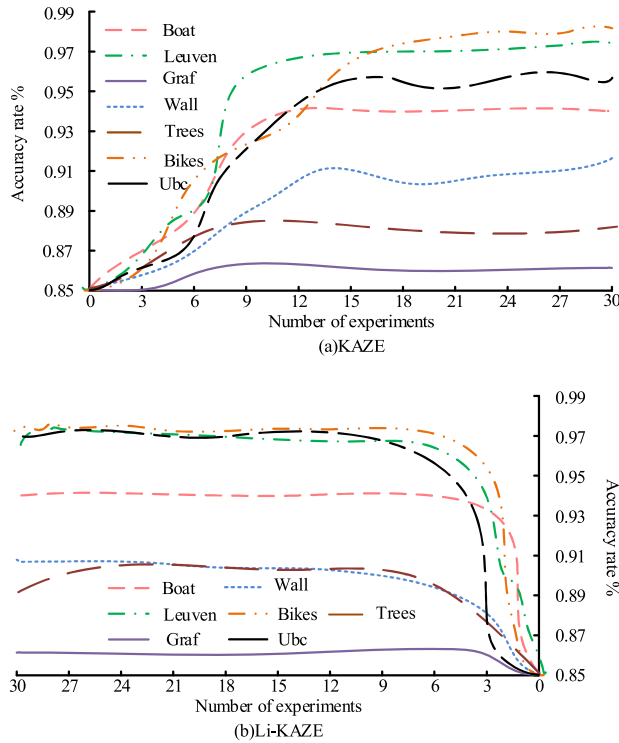


FIGURE 12. Comparison of algorithm matching accuracy.

average repeatability, and finally approaches zero infinitely. At this point, the change rates of all six algorithms have been improved accordingly, but the improved Li-KAZE algorithm still has the best performance, with an initial repeatability of 63%, higher than BRIEF's 40%, and the overall change trend is also the slowest among the comparison algorithms. Figure 14 shows the performance data of various algorithms that have changed the image perspective and illumination intensity.

In Figure 14 (a), the trend of changes in each algorithm is relatively rapid, while the change in BRIEF is relatively gentle. However, its highest repeatability is only 26%, so its overall performance is still the lowest. The initial repeatability of improved Li-KAZE reached 79%, which is still the highest among all algorithms. Except for BRIEF, this algorithm has a slower change speed compared to other algorithms. Therefore, Li-KAZE achieves the best performance when facing the wall with a changed perspective. In Figure 14(b), the change trends of each algorithm have shown corresponding improvements. The comprehensive repeatability of Li-KAZE is 77.8%, which is 57.6% higher than BRIEF. The trend of ORB change is the steepest, with a 45% difference between the maximum and minimum values. In summary, for the image group Leuven with varying brightness, the performance of the improved Li-KAZE algorithm is still the best. Figure 15 shows the performance experimental results of each algorithm when faced with changes in image compression size and comprehensive changes:

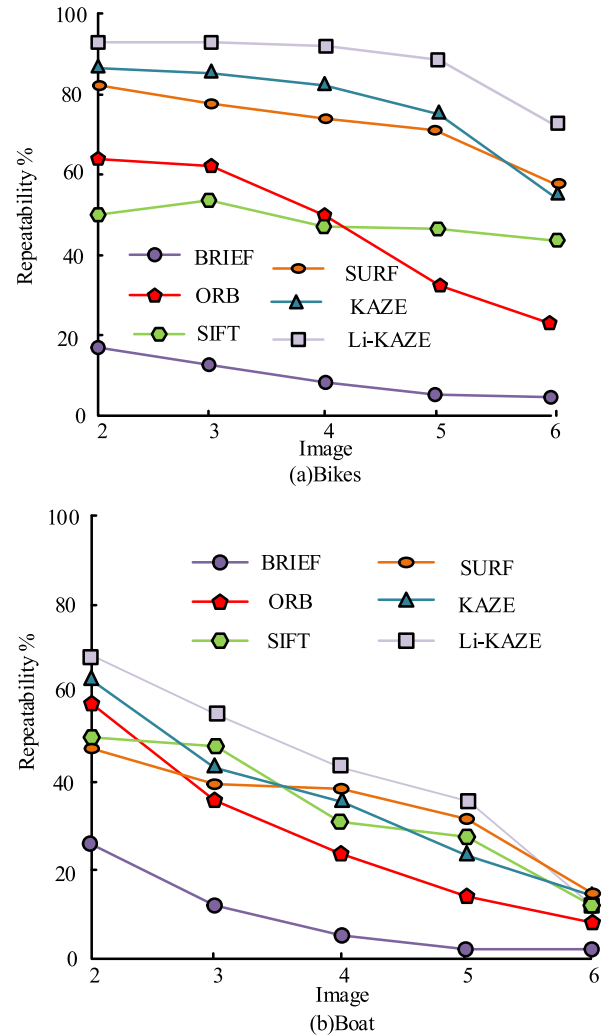


FIGURE 13. Image matching performance of each algorithm in clarity and scale.

In Figure 15(a), when confronted with a group of graphs with different compression values, the performance of the improved Li-KAZE and original KAZE algorithms is relatively good, with initial repeatability even approaching 100%, and the trend of change is relatively smooth. The average repeatability of the improved Li-KAZE was 94.6%. In Figure 15(a), the algorithms show a repeated upward and downward trend, and the repeatability values of Li-KAZE and original KAZE are still at relatively high values, with the highest and infinite approaching 100%. Based on the above experiments, the improving Li-KAZE can better perform image matching and achieve more efficient work when facing various changes in image groups. To further compare the comprehensive performance of each algorithm, the concept of performance matrix is introduced, which is four common indices of selection loss rate, accuracy, precision and recall rate [20]. At the same time, the UKbench dataset was introduced to conduct a performance control experiment, and the images were transformed by scale, smoothness, and

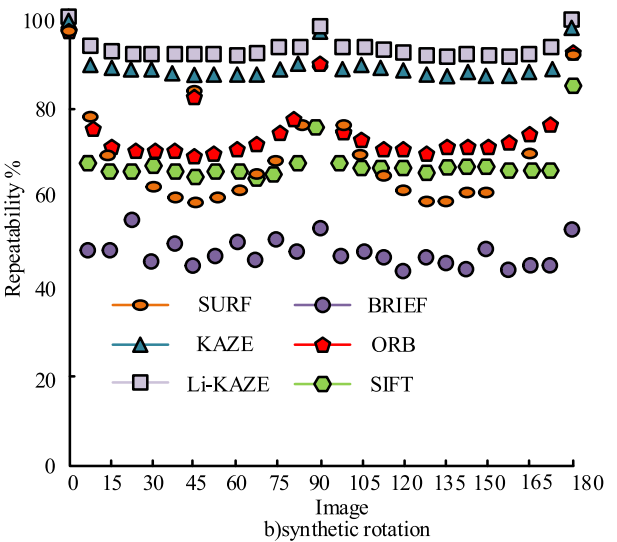
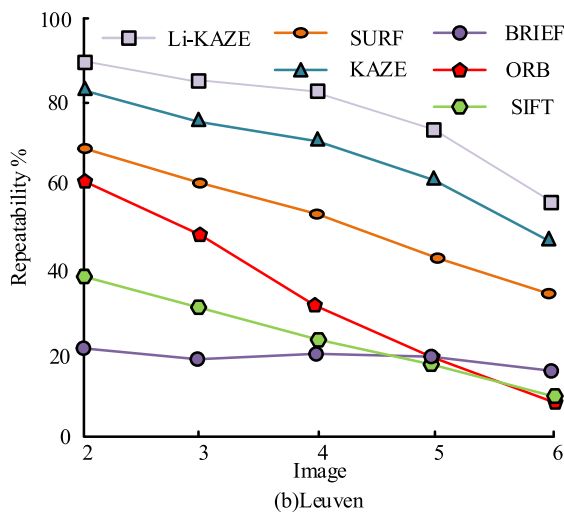
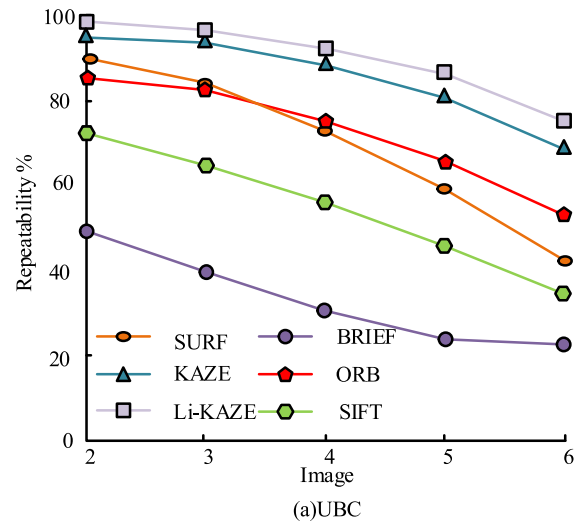
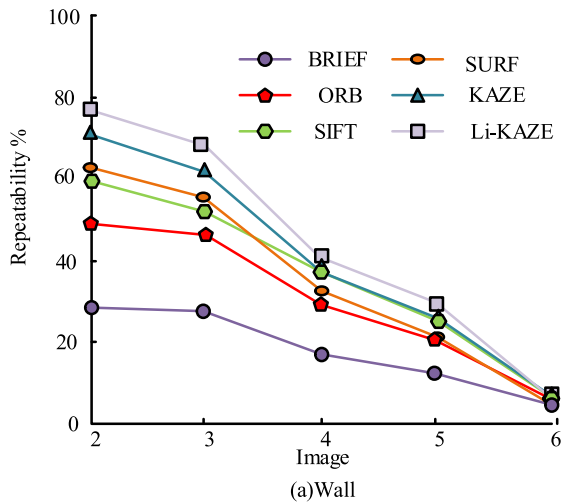


FIGURE 14. Image matching performance of each algorithm in image perspective and illumination intensity.

illumination, respectively. Due to the limitation of experimental cost, only Li-KAZE algorithm, SIFT algorithm, BRIEF algorithm and ORB algorithm were selected for analysis. The experimental results are shown in Figure 16.

From Figure 16 (a), it can be seen that the Li KAZE algorithm has the highest equilibrium point on the PR curve. This indicates that the Li KAZE optimization algorithm can achieve a better balance position compared to the ORB algorithm and SIFT algorithm, ensuring the accuracy and probability of precision of the model. As can be seen from Figure 16 (b), the final accuracy of Li-KAZE algorithm reaches 92.89%, while the final accuracy of ORB algorithm and SIFT algorithm are 87.51% and 79.83%, respectively. Compared with a decrease of 5.38% and 13.06%, the final loss rate of Li-KAZE algorithm is 1.23%, which is decreased by 0.07% and 0.12% compared with ORB algorithm and SIFT algorithm, respectively. Therefore, the overall performance of Li-KAZE algorithm is better. The above experiment uses a new data set and a new evaluation index to

FIGURE 15. Image matching performance of each algorithm on compression size and comprehensive change.

conduct further experiments on various algorithms, and the experimental results fully verify the excellent performance of Li-KAZE algorithm in various aspects. This improved algorithm greatly improves the operational efficiency and accuracy of image recognition, and can be applied to various fields such as criminal, medical and traffic image recognition technology. Because it can recognize all kinds of image deformation, it can still recognize better and faster, so it can be used for human life. Work provides great convenience. For example, the introduction of circular rotation and approximate Euclidean-style distance optimizes the timeliness of the image recognition model. At the same time, for the non-linear scale space, the additive operator splitting algorithm and Thomas fusion algorithm are used to improve the computational pressure, and the retention of detailed features is further optimized. Finally, the matching accuracy of the image matching model is realized when the scale changes and the compression rate changes are defects. In reference [21],

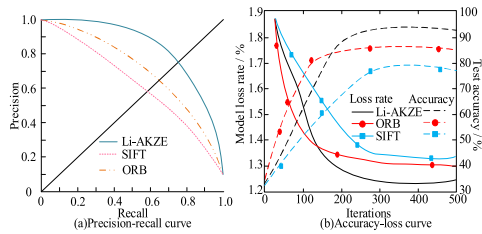


FIGURE 16. Comparison of PR curve and loss rate-accuracy curve of each algorithm.

it can be seen that the recognition accuracy of DenseNet201 and ResNet50 models is 92% and 83% respectively. By comparison, it can be seen that the model adopted in this study has the highest recognition accuracy, and the model is still faced with complex samples with image changes.

V. DISCUSSION

Various new concepts are introduced to optimize the original image matching algorithm, and good results are obtained, which contains the logic principle of matching optimization. According to the following experiment, the Li KAZE algorithm has the best comprehensive performance when facing transformations such as rotation, compression, and noise; And the algorithm has excellent performance in runtime, Precision, Recall curve, and accuracy loss rate curve. This is because the optimization algorithm adopts the characteristic of circular rotation. Instead of the original cumbersome main direction extraction, street distance and chessboard distance are introduced as approximate Euclidean distance, which greatly reduces the calculation amount. Therefore, the optimization model combines the advantages of each algorithm and solves their defects at the same time. In addition, to solve the complex problem of traditional nonlinear scale space computing, additive operator splitting and Thomas fusion algorithm are introduced to replace the inefficient forward Euler method. This further improves the efficiency of the model, better preserves the detailed features of the model, and enhances new feature attributes. Other matching algorithms may have various defects in computation time or feature extraction, so when there is a transformed or unclear image, these algorithms cannot identify the image well and perform correct matching.

VI. CONCLUSION

Image matching is an important component of image processing technology. In practical applications, images are often affected by scale changes, compression, and noise. Therefore, how to eliminate irrelevant factors during image matching is the key to achieving efficient image matching. This study proposes an improved Li-KAZE algorithm, which also uses a nonlinear scale space that can handle image edges and details well, and introduces 2ndODV and expected distance to improve the algorithm's computational speed. The original main direction extraction is replaced by the circular rotation

characteristic, which avoids the inconvenience caused by a large number of traversing data. At the same time, the geometric sum of chessboard distance and street distance is used to replace the original feature matching process, which greatly reduces the computational burden of the algorithm. Finally, this study conducted multiple simulation experiments on the improved algorithm and other ORB algorithms. Experiments have shown that the improved Li-KAZE has little difference in the number of extracted features and matching accuracy compared to the original KAZE, but there is a significant improvement in the speed of feature extraction and matching. The average feature extraction time of Li-KAZE is 2.33s, which is a decrease of 0.1s compared to the original KAZE; When performing feature matching, the average feature matching time of Li-KAZE is 1.57s, while for Bikes, the matching time is only 1s. The average matching time is reduced by 1.44 seconds compared to the original algorithm. In comparison with other SIFT and other algorithms, Li-KAZE has always been the best performing of all algorithms. In Leuven, where the noise was changed, the repeatability of Li-KAZE increased by 57.6% compared to BRIEF; In Ubc, the average repeatability of Li-KAZE even reached 94.6%. In summary, the improvement of Li-KAZE has shorter computation time and higher efficiency, which can achieve better image matching functions. Compared with other algorithms, the image matching ability of the proposed algorithm in the face of feature changes has been further improved, especially some complex fuzzy changes, and better image matching effect can be achieved. However, this algorithm still has some shortcomings. When it is applied to video image matching, Li-KAZE algorithm cannot fully realize the correct tracking of each frame in the face of small target tracking, and the error of the previous frame will lead to the error of the next frame, so that the subsequent research needs to introduce other algorithms or mechanisms for optimization. At the same time, compared with the original algorithm, although the real-time performance of the optimization algorithm has been improved, its performance changes are not significant enough. In future research, it is necessary to strengthen the improvement of recognition performance on the basis of maintaining timeliness.

REFERENCES

- [1] F. Masood, J. Masood, and H. Zahir, "Novel approach to evaluate classification algorithms and feature selection filter algorithms using medical data," *J. Comput. Cognit. Eng.*, vol. 2, no. 1, pp. 57–67, 2023.
- [2] J. L. Zhong, Y. F. Gan, C. M. Vong, J. X. Yang, and J. H. Luo, "Effective and efficient pixel-level detection for diverse video copy-move forgery types," *Pattern Recognit.*, vol. 122, no. 2, 2021, Art. no. 108286.
- [3] Q. Liu, X. Xi, W. Zhang, L. Yang, and N. Hanajima, "Improved image matching algorithm based on LK optical flow and grid motion statistics," *Int. J. Comput. Appl. Technol.*, vol. 68, no. 1, pp. 49–57, 2022.
- [4] T. A. Al-Shurbaji, K. A. AlKaabneh, I. Alhadid, and R. Masa'deh, "An optimized scale-invariant feature transform using chamfer distance in image matching," *Intell. Autom. Soft Comput.*, vol. 31, no. 2, pp. 971–985, 2022.
- [5] H. Yan, Y. Wang, Y. F. Wang, and Y. G. Zhou, "Electrical capacitance tomography image reconstruction by improved orthogonal matching pursuit algorithm," *IET Sci., Meas. Technol.*, vol. 14, no. 3, pp. 367–375, May 2020.

- [6] J. Yue, S.-L. Gao, F.-M. Li, and N.-B. Cai, "Fast image matching algorithm with approximate affine area detection and scale invariance," *Opt. Precis. Eng.*, vol. 28, no. 10, pp. 2349–2359, 2020.
- [7] W. Li, X. Na, P. Su, Y. Lu, and T. Dong, "A novel image matching algorithm based on PCA and SIFT," *J. Phys., Conf. Ser.*, vol. 1684, no. 1, pp. 012099–012107, 2020.
- [8] J. Liang, K. Xiao, and G. Gao, "A depth-colour image registration method based on local feature point extraction," *Biosystems Eng.*, vol. 219, pp. 268–280, Jul. 2022.
- [9] S. Ji, C. Zeng, Y. Zhang, and Y. Duan, "An evaluation of conventional and deep learning-based image-matching methods on diverse datasets," *Photogrammetric Rec.*, vol. 38, no. 182, pp. 137–159, 2023.
- [10] R. Qian, Y. Zhao, R. Feng, W. Yang, and Z. Zhang, "An algorithm for single view occlusion area detection in binocular stereo matching," *Int. J. Pattern Recognit. Artif. Intell.*, vol. 37, no. 2, Feb. 2023, Art. no. 2350003.
- [11] P. Chevalier, P. Quéméré, S. Bérard-Bergery, J.-B. Henry, C. Beylier, and J. Vaillant, "Rigorous model-based mask data preparation algorithm applied to grayscale lithography for the patterning at the micrometer scale," *J. Microelectromech. Syst.*, vol. 30, no. 3, pp. 442–455, Jun. 2023.
- [12] S. W. Hwang, T. Lee, H. Kim, J. G. Choi, and H. Yeo, "Classification of wood knots using artificial neural networks with texture and local feature-based image descriptors," *Holzforschung*, vol. 76, no. 1, pp. 51–65, 2021.
- [13] L. Zhang, K. Li, Y. Qi, and F. Wang, "Local feature extracted by the improved bag of features method for person re-identification," *Neurocomputing*, vol. 458, pp. 690–700, Oct. 2021.
- [14] A. Fejér, Z. Nagy, J. Benois-Pineau, P. Szolgay, A. de Ruyg, and J. Domenger, "Implementation of scale invariant feature transform detector on FPGA for low-power wearable devices for prostheses control," *Int. J. Circuit Theory Appl.*, vol. 49, no. 7, pp. 2255–2273, Jul. 2021.
- [15] H. Gao and Q. Chen, "A robust and secure image watermarking scheme using SURF and improved artificial bee colony algorithm in DWT domain," *Optik*, vol. 242, no. 10, 2021, Art. no. 166954.
- [16] D. Senthilkumar and R. Arulmurugan, "Gaussian bilateral filtered discrete Hartley feature transformation based infomax boosting for hyperspectral image classification," *Int. J. Intell. Netw.*, vol. 2, no. 1, pp. 195–203, 2021.
- [17] B. Hedelin, S. Gray, S. Woehlke, T. K. Bendor, and E. Sterling, "What's left before participatory modeling can fully support real-world environmental planning processes: A case study review," *Environ. Model. Softw.*, vol. 143, no. 2, 2021, Art. no. 105073.
- [18] S. Ma, P. Guo, H. You, P. He, G. Li, and H. Li, "An image matching optimization algorithm based on pixel shift clustering RANSAC," *Inf. Sci.*, vol. 562, pp. 452–474, Jul. 2021.
- [19] D. Li, Q. Xu, W. Yu, and B. Wang, "SRP-AKAZE: An improved accelerated Kaze algorithm based on sparse random projection," *IET Comput. Vis.*, vol. 14, no. 4, pp. 131–137, Jun. 2020.
- [20] U. Kutbay, "Automated hemangioma detection using Otsu based binarized Kaze features," *Multimedia Tools Appl.*, vol. 79, nos. 33–34, pp. 24781–24793, Sep. 2020.
- [21] F. Yasmin, Md. M. Hassan, M. Hasan, S. Zaman, C. Kaushal, W. El-Shafai, and N. F. Soliman, "PoxNet22: A fine-tuned model for the classification of monkeypox disease using transfer learning," *IEEE Access*, vol. 11, pp. 24053–24076, 2023.



PEIPEI ZHANG was born in Shandong, China, in 1988. She received the B.S. degree in electronic information engineering from Dezhou University, Shandong, in 2011, and the M.S. degree in communication and information systems from Shandong University, Shandong, in 2014.

Since 2020, she has been an Associate Professor with the Xi'an Traffic Engineering Institute. She has published more than ten core and above academic articles. Her research interests include

image processing and target recognition.



XINE YAN was born in Hubei, China, in 1981. She received the B.S. degree in civil engineering from the Hubei University of Technology, Hubei, in 2004, and the M.S. degree in structural engineering from the Xi'an University of Architecture and Technology, Shaanxi, China, in 2009.

From 2004 to 2009, she was a Teaching Assistant with the School of Human Settlements and Environment, Xi'an Eurasian University, Shaanxi.

Since 2010, she has been a Lecturer with the School of Human Settlements and Environment, Xi'an Eurasian University. Until 2017, she was an Associate Professor with the School of Human Settlements and Environment, Xi'an Eurasian University. Since 2019, she has been with the School of Civil Engineering, Xi'an Institute of Transportation Engineering, and was appointed as a Professor, in 2021. She is the author of two books and more than 20 articles. Her research interests include building materials, green construction, and intelligent construction.

...